Nano World Journal

https://doi.org/10.17756/nwj.2023-s1-119

Research Article

Open Access

Structural Optimization for Effective Damping Force of a Magneto-rheological Damper for High Velocity Application

M.B. Kumbhar[1*], R.G. Desavale[2] and T. Jagadeesha[3]

[1]*Mechanical Engineering Department, Department of Technology, Shivaji University, Kolhapur, Maharashtra, India*
[2]*Mechanical Engineering Department, Rajarambapu Institute of Technology, Shivaji University, Rajaramnagar, Kolhapur, Maharashtra, India*
[3]*Mechanical Engineering Department, National Institute of Technology, Calicut, Kozhikode, Kerala, India*

[*]Correspondence to:
M.B. Kumbhar
Mechanical Engineering Department,
Department of Technology, Shivaji University,
Kolhapur, Maharashtra, India.
E-mail: mkumbhar44@gmail.com

Received: November 24, 2022
Accepted: May 18, 2023
Published: May 20, 2023

Citation: Kumbhar MB, Desavale RG, Jagadeesha T. 2023. Structural Optimization for Effective Damping Force of a Magneto-rheological Damper for High Velocity Application. *NanoWorld J* 9(S1): S615-S620.

Published by United Scientific Group

Abstract

The twin-tube dampers are more popular due to their outstanding controlling and regulation qualities in most driving conditions with cost-effective. Magneto-rheological (MR) dampers are used in automotive applications to boost damping force while maintaining geometric constraints. Two significant parameters considered while evaluating an MR damper's efficiency are valve ratio and controllable force. These parameters are used to define a geometric configuration of an MR damper. The effective damping force increases according to the magnetic field strength. The magnetic circuit analysis reveals that the damping force is directly proportional to the applied current. The proposed model can significantly improve the suspension damping effect for high-speed applications.

Keywords

Magneto-rheological damper, Twin tube, Valve ratio, Controllable force, Damping force

Introduction

Numerous preceding analytical studies in viscous damper suspensions were evaluated using semiactive MR approaches. They were discovered to have good characteristics and efficient control systems [1]. Due to the superior dynamic properties such as rapid response, resistant environmental features, max strength, low energy consumption, simple electrical feedback and mechanical output connections and an exceptional capacity and unique nature of MR fluid [2-7]. Developing novel MR dampers for various applications, including absorbing enormous loads in aerial and terrestrial vehicles depends on these fluids' suitability for custom flow control [8]. Studies and applications of the MR fluid damper technology include shock absorbers [1, 9], clutches, brakes [10], hydraulic valves, railway vehicles, actuators, gun recoil systems [11, 12], polishing devices, military suspension systems, civil infrastructure seismic isolation systems [2, 13, 14], flight control, avionics, energy conversion and other fields [15], the prosthetic leg, lower-limb exoskeleton [16], human shoulder rehabilitation ball, and socket damper [17].

Twin-tube and mono-tube dampers are the most popular and commercial MR damper types [18]. Single-coil annular valve, double-coil annular valve, triple-coil annular valve, and annular radial valve geometrical dimensions were optimised. The goal function was to optimize the valve ratio. It was determined that the MR valve with two coils offered the best valve ratio, while the annular radial-type valve provided the best pressure drop [19]. Developed, and simulated a rapid response MR valve this was accomplished by precisely developing the active zone and adopting ferrite material for the magnetic circuit [20]. It was

revealed that the geometrical arrangements of the fluid flow channel and coil designs play an important influence in determining the effective zone within the valve [21]. There are very few examples in the literature where a twin-tube MR damper was developed for; the valve ratio and the controlled force to consider when evaluating an MR damper's efficiency. Most of the MR dampers were not for effective damping force. Also, the damping forces developed by these prototypes were insufficient for effective tuning to control the vibration. These parameters are determined by the number of holes (n), valve holes pitch circle diameter (t_h), flange thickness (t_f), and valve hole diameter (t_g). The impact force should be absorbed more slowly and steadily to maximize efficiency. Structural optimization has been provided to increase rider comfort and safety.

Twin Tube MR Damper Mathematical Modeling

For valve mode simplification, the flow is modeled as if it were a flow among the two adjacent plates, because the damping force is linear, and the gap's height is considerably lower than its length and width as shown in figure 1. Stress value is constant along the gap, and magnetic flux in the gap. Piston assembly magnetic coil housed in it and has holes for flow through of fluid, the magnetic fluid controls fluid rheology in the annular gap, driven either by displacement (or) applied to main piston rod $x_r(t)$, $v_r(t)$ or cylinder $x_t(t)$, $v_t(t)$. Thus, piston rod's relative displacement and cylinder is:

$$x_p = x_r - x_t$$

Let, Q_{v1} flow with across the piston annular gap, L the annular path's length, and A_g and Q_{v2} are the cross-sectional areas. Net foot valve flow plus the piston pressure drop is calculated.

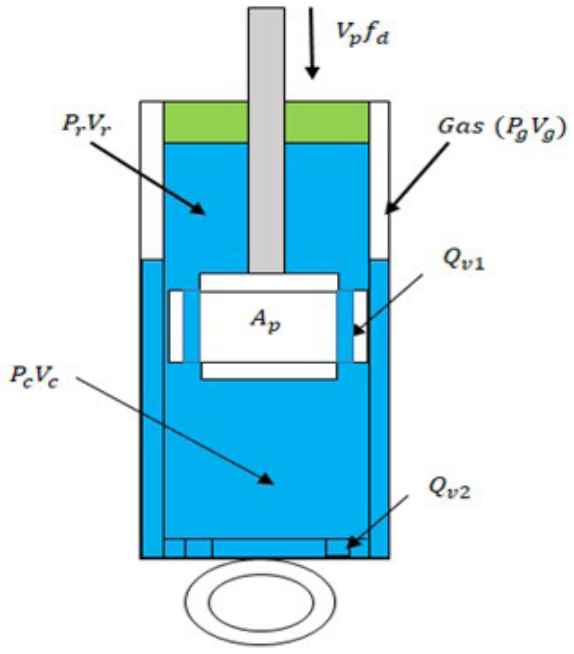

Figure 1: MR damper.

$$\Delta P = P_r - P_c \tag{1}$$

Where, P_r = Recoil cylinder pressure and P_c = Compression cylinder pressure

The bulk modulus of elasticity is,

$$\hat{a}_i = -V\frac{dP}{dV}$$

The equation for isothermal compressibility is,

$$C_f V\frac{dP}{dV}$$

The volume of the rebound and compression chambers.

$$\frac{dV}{dt} = \sum Q_{in} - \sum Q_{out}$$

Substituting value of $\frac{dV}{dt}$ as follows,

$$C_f V\frac{dV}{dt} = \frac{\hat{a}_f}{V}\left(\sum Q_{in} - \sum Q_{out}\right) \tag{2}$$

where, β_f = container's stiffness, and $\beta_{c'}$ = pressure expands the cylinder walls.

The following relationship was constructed using the fluid bulk modulus and the volumetric effect together:

$$\frac{1}{\hat{a}} = \frac{1}{\hat{a}_f} + \frac{1}{\hat{a}_C} \tag{3}$$

Taking into account the cylinder material's compliance,

$$\frac{1}{\hat{a}_C} = \frac{1}{E_S}\left(v - \frac{D_o^2 + D_P^2}{D_L^2 - D_P^2}\right)$$

The gas compressibility is,

$$\hat{a}_f(P) = \hat{a}_O \frac{1 + K\left(\frac{P_a}{P_a + P}\right)^{\frac{1}{n}}}{1 + K\frac{P_a^{\frac{1}{n}}}{n(P_a + P)^{\frac{1+n}{n}}}} \tag{4}$$

Let, V_r and V_c the volume of the rebound and compression chambers, respectively.

$$V_r = V_{ro} + (A_p - A_r)x_p \tag{5}$$

$$V_c = V_{co} - A_p x_p \tag{6}$$

Rebound pressure variations can be calculated using equation (3) as follows:

$$P_r = \frac{\hat{a}}{V_r}\left[(A_p - A_r)V_p - Q_{v1}\right] \tag{7}$$

Furthermore, pressure changes in the compression chamber as a result of:

$$P_c \frac{V_c}{\hat{a}} = \frac{\hat{a}}{V_c}\left[-A_p V_p + Q_{v1} + Q_{v2}\right] \quad (8)$$

Where, V_p = Piston velocity

By imposing constraints on the flow, i.e., $P_r \geq P_v$ and $P_c \geq P_v$, when the fluid mass inside the damper's annular gap is moving, however:

$$\ddot{A}P \times A = \tilde{n}L\dot{Q}$$

As a result, there is flow through valve holes:

$$\hat{Q}P_{v1} = \frac{A_g}{\tilde{n}_L}\left(P_r - P_c - \quad_a\right) \quad (9)$$

Assuming that the process pressure is adiabatic due to the presence of gas:

$$P_g\left(V_{go} - \int Q_{v2}dt\right)^n = P_{go}\left(V_{go}\right)^n$$

$$P_g = P_{go}\left(\frac{V_{go}}{V_{go} - \int Q_{v2}dt}\right)^n \quad (10)$$

The foot valve that is used to drain the water is provided by,

$$Q = C_d A\sqrt{2\frac{\Delta P}{\tilde{n}\left(1 - \frac{D_g}{D_p}\right)}}$$

$$\Delta P = P_r - P_c, \quad \frac{D_g}{D_p} \cong 0$$

$$Q_{v2} = C_d A\sqrt{2\frac{P_r - P_c}{\tilde{n}}} \quad (11)$$

The dampening force is illustrated as:

$$F_d = F_f + \left(A_p - A_r\right)P_r - A_p P_c \quad (12)$$

Where, F_d = frictional force

MR Damper Flow Valve Optimization

Flow chart for a structural optimization MR damper for effective damping force in a high velocity application, as shown in figure 2. Consider a cylinder with a radius of 35 mm and a valve hole with a diameter of length of 50 mm. The MR fluids post-yield viscosity is believed to be fixed which is, 0.092 Pas and The MR valves have a flow rate of Q = 3E-4 m^3/s. The following parameters are considered to achieve better a damping:

- Number of holes (n)
- Valve hole PCD in mm (t_h)

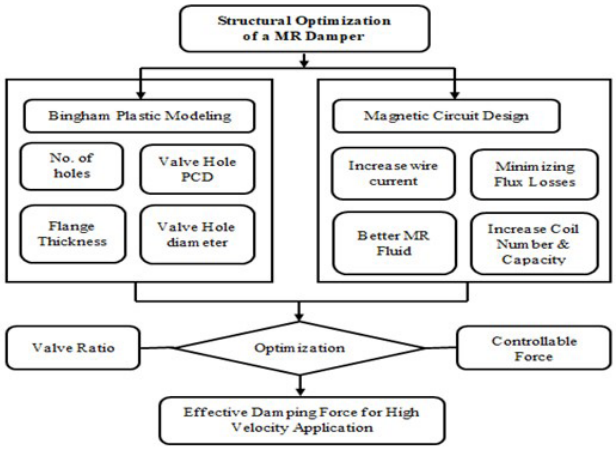

Figure 2: Flow chart for a structural optimization MR damper.

- flange thickness in mm (t_f)
- the valve holes diameter in mm (t_g)

It is a multi-variable optimization problem and can be solved using appropriate methods. However, the procedure is complete and lengthy. One way is to develop a MATLAB program and using a trial-and-error method, the appropriate values of desired parameters for optimization of the valve ratio and the controlled force was modified by examining the relationship between the (n, t_h, t_f, t_g). Observations/inferences made out of these graphs are as follows:

Number of holes

Here, t_h = 0.0025 m, t_f = 0.005 m, and t_g = 0.003 m.

Figure 3 shows the relationship between valve ratio and applied current for various hole counts. As the number of valve holes rises, the magnetic field reveals more MR fluid including the pressure difference between chambers. However, due to design considerations, the number of holes that can be added is limited.

Diameter of pitch circle

MHere, n = 0.003 m, t_f = 0.005 m, and t_g = 0.003 m.

Figure 4 shows the relationship between the valve ratios with an applied current for various PCD. It demonstrates that a little modification in the pitch circle diameter does not influence the valve ratio. As a result, it was concluded to take design strength and wear into consideration.

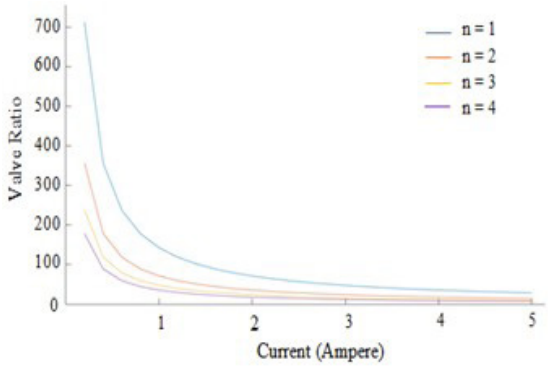

Figure 3: Optimization of number of holes.

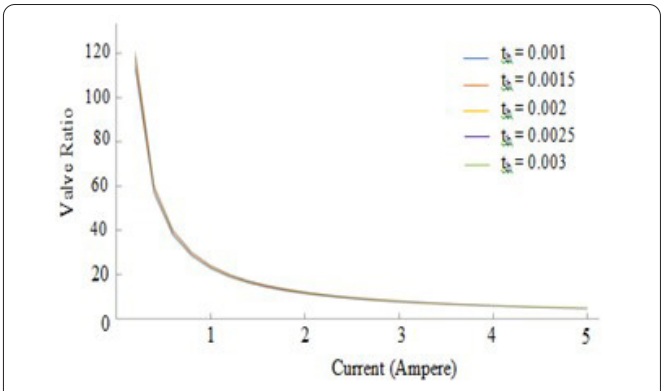

Figure 4: Optimization of pitch circle.

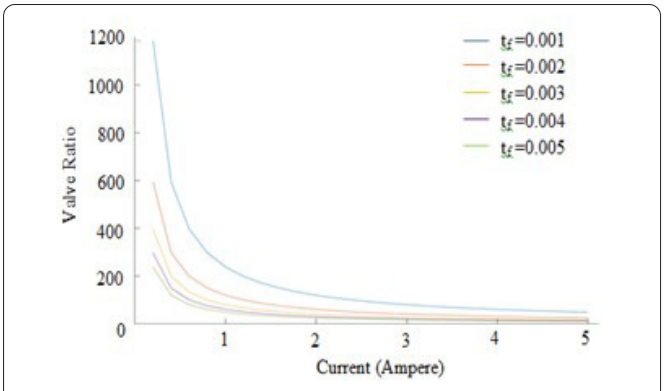

Figure 5: Optimization of flange thickness.

Flange thickness

Here, n = 0.003 m, t_h = 0.0025 m, and t_g = 0.003 m.

Figure 5 shows the variation in valve ratio with an applied current for various flange thicknesses. The valve ratio decreases as flange thickness increases, because under magnetic influence, the MR fluid flow length area increases.

Diameter of valve holes

Here, n = 0.003 m, t_h = 0.0025 m, and t_f = 0.005 m.

Figure 6 shows the variation of valve ratio with the current for multiple valve hole diameters. Due to uncontrolled force, the valve ratio drops as the pressure changes along the valve holes diminishes.

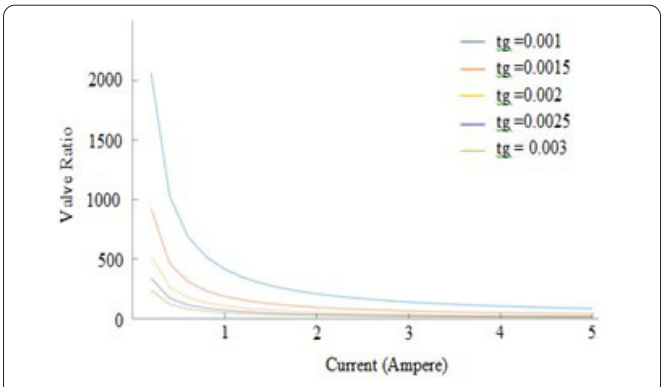

Figure 6: Optimization of diameter of valve holes.

Based on the observations made thus far, it has been determined that the minimum value of valve ratio can be constrained by the following:

While designing, the best plot was found by trial-and-error method in the above given range of the parameters and strength into account as shown in table 1. The inference found out from the graphs is also taken into consideration. The dimensions of the parameters are: The total number of holes 3; Pitch circle diameter 3.5 mm; Thickness of flange 5 mm; Valve holes diameter 3 mm. Figure 7 shows the optimized curve for valve ratio with applied current.

Optimization of a magnetic field for the magnetic circuit

There are several ways to improve MR damper performance: increasing wire current, increasing coil capacity and number, utilizing a better MR fluid, and minimizing flux loss [4, 17, 19]. A magnetic field and north and south pole are generated inside a coil when electricity is applied to it. A magnetic field's intensity is:

$$B = \mu_0 \frac{N}{L} I$$

Where, μ_0 is air permeability, N is number of turns, L is winding length, and I is input current.

The number of turns is thus,

$$N = \frac{BL}{\mu_0 I}$$

Considering, B = 1 Tesla, L = 5E-2 m, and I = 5 amps, 60% tangential efficiency, and number of turns is 12732. Consider a TWG rated wire with a 0.25 mm diameter and a maximum current of 5 A. Dividing the armature core's length by the thickness of the winding wire yields the number of turns per plane or layer. Each layer contains 172 turns. The wire thickness was divided by the allowed winding radius for each layer. 40 layers of winding thus, the armature core might have 6880 turns. The designed armature core can produce roughly 0.54 T at 5 A; it is approximately 54% of the overall windings.

Armature core analysis for magnetic circuit

Compute the magnetic flux density at the piston, armature core, and MR fluid. 6000 coil windings energize the MR liquid. The current through the coils changes because MR dampers affect flux density.

Figure 8 shows that the nodal solution and magnetic field lines intersect the piston. The line spacing indicates the magnetic field strength. Collinear lines are more intense. The piston's fluid flow follows the field lines. The control strategy

Table 1: The optimized value of valve ratio.

The total number of holes	3 - 5
Pitch circle diameter (mm)	2.5 - 4
Thickness of flange (mm)	>= 5
Valve holes diameter (mm)	3 - 6

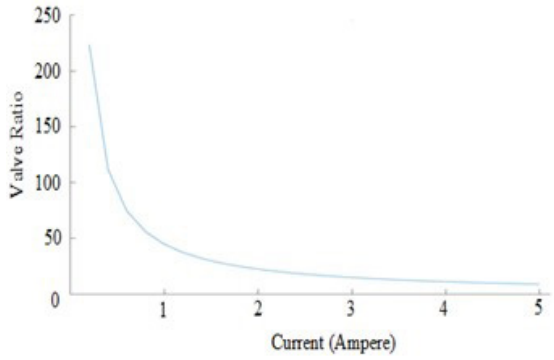

Figure 7: Optimized curve for valve ratio with applied current.

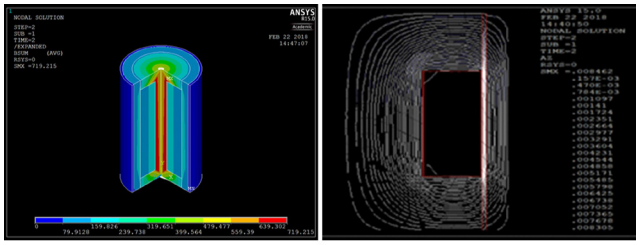

Figure 8: (a) Nodal solution and **(b)** Magnetic field lines.

affects the damping force, which is controlled by an applied magnetic field. It also ensures that magnetic flux goes perpendicularly through the MR fluid. To reduce energy consumption by implementing more electromagnetic coils with low current and appropriate management techniques should be utilized to allow the impact force to buffer more slowly and steadily.

Conclusion

Valve hole size has an inverse relationship with controlled force; however, to enhance the effectiveness of the MR damper, the regulated force should be as large as possible. As a result, microscopic valve holes must be drilled. The valve ratio decreases as the number of valve holes, flange thickness, and hole diameter increase. The MR effect will be modeled under severe flow conditions. When a magnetic field is introduced, the MR effect occurs, resulting in yield stress. The MR effect varies with the magnetic field strength. Thus, optimizing magnetic circuit designs for valve ratio and variable force is responsible for many applications. To absorb heavy loads and high-velocity effects efficiently, this modeling for structural optimization must be exact and consistent with the ideal control method for the maximum damping force.

Acknowledgements

None.

Conflict of Interest

The authors declare that they have no conflict of interest regarding the publication of this article.

Credit Author Statement

M.B. Kumbhar: Conceptualization, Methodology, Formal analysis; R.G. Desavale: Writing - review and editing, Supervision; T. Jagadeesha: Writing - review and editing. All the authors read and approved the manuscript.

References

1. Fujitani H, Sodeyama H, Hata K, Komatsu Y, Iwata N, et al. 2002. Dynamic performance evaluation of 200kN magnetorheological damper. *Tech Note Natl Inst Land Infrastruct Manag* 41: 349-356.
2. Zhu X, Jing X, Cheng L. 2012. Magnetorheological fluid dampers: a review on structure design and analysis. *J Intell Mater Syst Struct* 23(8): 839-873. https://doi.org/10.1177/1045389X12436735
3. Khan SA, Suresh A, Seetharamaiah N. 2014. Principles, characteristics and applications of magneto rheological fluid damper in flow and shear mode. *Procedia Mater Sci* 6: 1547-1556. https://doi.org/10.1016/j.mspro.2014.07.136
4. Zheng J, Li Z, Koo J, Wang J. 2014. Magnetic circuit design and multiphysics analysis of a novel MR damper for applications under high velocity. *Adv Mech Eng* 6: 402501. https://doi.org/10.1155/2014/402501
5. Huang L, Li J, Zhu W. 2017. Mathematical model of a novel small magnetorheological damper by using outer magnetic field. *AIP Adv* 7(3): 035114. https://doi.org/10.1063/1.4978866
6. Qian C, Yin X, Ouyang Q. 2021. Modeling and parameter identification of the MR damper based on LS-SVM. *Int J Aerosp Eng* 2021: 6648749. https://doi.org/10.1155/2021/6648749
7. Gołdasz J, Sapiński B. 2015. Insight into Magnetorheological Shock Absorbers. Springer Cham.
8. Siginer DA, Letelier MF, Stockle J. 2021. A new approach to the modeling of magnetorheological dampers and application to resonance control. *J Fluids Eng* 143(9): 091504. https://doi.org/10.1115/1.4050513
9. Chooi WW, Oyadiji SO. 2009. Experimental testing and validation of a magnetorheological (MR) damper model. *J Vib Acoust* 131(6): 061003. https://doi.org/10.1115/1.3142885
10. Bai XXF, Sedaghati R, Goldasz J, Sun S. 2021. Hysteresis characterization and control of electrorheological and magnetorheological materials. *Front Mater* 8: 732353. https://doi.org/10.3389/fmats.2021.732353
11. Kumbhar MB, Salunkhe VG, Borgaonkar AV, Jagadeesha T. 2021. Mathematical modeling and experimental evaluation of an air spring–air damper dynamic vibration absorber. *J Vib Eng Technol* 9: 781-789. https://doi.org/10.1007/s42417-020-00263-w
12. Shiao Y, Kuo WH, Nguyen QA, Lai CW. 2015. Development of a variable-damping magnetorheological damper with multiple poles. *J Vibroeng* 17(3): 1071-1078.
13. Ahamed R, Ferdaus MM, Li Y. 2016. Advancement in energy harvesting magneto-rheological fluid damper: a review. *Korea Aust Rheol J* 28: 355-379. https://doi.org/10.1007/s13367-016-0035-2
14. Rahman M, Ong ZC, Julai S, Ferdaus MM, Ahamed R. 2017. A review of advances in magnetorheological dampers: their design optimization and applications. *J Zhejiang Univ Sci A* 18(12): 991-1010.
15. Yang W. 2017. Magnetic levitation force exerted on the cylindrical magnet in a ferrofluid damper. *J Vib Control* 23(14): 2345-2354. https://doi.org/10.1177/1077546315616516
16. Phu DX, Choi SB. 2019. Magnetorheological fluid based devices reported in 2013–2018: mini-review and comment on structural configurations. *Front Mater* 6: 19. https://doi.org/10.3389/fmats.2019.00019
17. El Wahed AK, Wang HC. 2019. Performance evaluation of a magnetorheological fluid damper using numerical and theoretical methods with experimental validation. *Front Mater* 6: 27. https://doi.org/10.3389/fmats.2019.00027

18. Lv H, Zhang S, Sun Q, Chen R, Zhang WJ. 2021. The dynamic models, control strategies and applications for magnetorheological damping systems: a systematic review. *J Vib Eng Technol* 9: 131-147. https://doi.org/10.1007/s42417-020-00215-4

19. Nguyen QH, Han YM, Choi SB, Wereley NM. 2007. Geometry optimization of MR valves constrained in a specific volume using the finite element method. *Smart Mater Struct* 16(6): 2242. https://doi.org/10.1088/0964-1726/16/6/027

20. Kubík M, Macháček O, Strecker Z, Roupec J, Mazůrek I. 2017. Design and testing of magnetorheological valve with fast force response time and great dynamic force range. *Smart Mater Struct* 26(4): 047002. https://doi.org/10.1088/1361-665X/aa6066

21. Abd Fatah AY, Mazlan SA, Koga T, Zamzuri H, Zeinali M, et al. 2015. A review of design and modeling of magnetorheological valve. *Int J Modern Phys B* 29(04): 1530004. https://doi.org/10.1142/S0217979215300042